50 Gb/s PAM4 underwater wireless optical communication systems across the water–air–water interface [Invited]

Chung-Yi Li (李忠益)[1], Hai-Han Lu (呂海涵)[2,*], Yong-Cheng Huang (黃永程)[2], Qi-Ping Huang (黃期平)[2], Jing-Yan Xie (謝景硯)[2], and Song-En Tsai (蔡松恩)[2]

[1]*Department of Communication Engineering, Taipei University, New Taipei City 237, China*
[2]*Institute of Electro-Optical Engineering, Taipei University of Technology, Taipei 106, China*
**Corresponding author: hhlu@ntut.edu.tw*

Received June 17, 2019; accepted September 5, 2019; posted online September 27, 2019

A 50 Gb/s four-level pulse amplitude modulation (PAM4) underwater wireless optical communication (UWOC) system across the water–air–water interface is demonstrated in practice. In practical scenarios, laser beam misalignment due to oceanic turbulence degrades performance in UWOC systems. With the adoption of a reflective spatial light modulator (SLM) with an electrical controller, not only can the laser be arbitrarily adjusted to attain a water–air–water scenario, but oceanic engineering problems can also be resolved to establish a reliable UWOC link. Brilliant bit error rate performance and clear PAM4 eye diagrams are attained by adopting a Keplerian beam expander and a reflective SLM with an electrical controller. This proposed PAM4 UWOC system presents a feasible state that outperforms existing UWOC systems due to its feature providing a high-speed water–air–water link.

OCIS codes: 010.3310, 010.7340, 060.4510, 140.7300.
doi: 10.3788/COL201917.100004.

Underwater wireless optical communication (UWOC) systems are used to deliver data in an unguided water environment through laser beams. In comparison with acoustic and radio frequency (RF)-based underwater wireless communication (UWC) systems, laser-based UWOC systems have an extensively higher transmission bandwidth, and hence provide a significantly higher transmission capacity. Laser-based UWOC systems have attracted extensive attention in recent years because of such a large transmission capacity advantage[1–7]. In the domain of UWOC systems, researchers mostly aim to construct high-transmission-rate UWOC systems across the air–water–air interface. However, air–water–air interface does not exist in a practical scenario, as the laser beam should escape (upstream) or enter (downstream) from the top of the water tank[8,9]. Therefore, this demonstration illustrates a 50 Gb/s four-level pulse amplitude modulation (PAM4) UWOC system across the water–air–water interface. An uplink from water to air and a downlink from air to water are established in practice. For the first time, a 50 Gb/s PAM4 UWOC system is feasibly constructed with the adoption of a reflective spatial light modulator (SLM) and an electrical controller. The reflective SLM functions as a flexible mirror through the electrical controller[10]. In practical scenarios, a laser beam misalignment on account of natural wind in the environment will lead to performance degradation and link unreliability. To mitigate these problems, a reflective SLM with an electrical controller is adopted, which not only allows the laser beam to be reflected to develop a practical water–air–water scenario, but also conquers oceanic engineering problems to construct a reliable UWOC link. Regarding temperature variation, laser misalignment because of temperature turbulence will introduce signal fading[11]. Therefore, the water temperature is kept at 20°C throughout the experiment to avoid unnecessary variation.

Wang *et al.* achieved an adaptive water–air–water data information transfer with orbital angular momentum (total bit rate of 1.08 Gb/s)[8]. Chen *et al.* demonstrated a 26 m/5.5 Gb/s air–water optical wireless link with both downlink and uplink transmissions[12]. Wang *et al.* illustrated a 100 m/500 Mb/s UWOC system using a 520 nm green-light laser diode (LD)[13]. Nevertheless, the data rate of 1.08 Gb/s/5.5 Gb/s/500 Mb/s is far lower than the related rate of 50 Gb/s transmitted in this proposal. In addition, the air–water–air interface does not meet the target of practical scenarios. Islam *et al.* established a UWOC link through the air–water interface using multiple blue-light light-emitting diodes (LEDs)[9]. Nonetheless, the transmission rate and transmission distance of UWOC links are restricted due to the LEDs' bandwidth limitation. In this study, a feasible 50 Gb/s PAM4 UWOC system with a reflective SLM is demonstrated. Excellent bit error rate (BER) performance and clear PAM4 eye diagrams are attained through the water–air–water interface. It presents a practical scenario that outperforms existing UWOC systems by providing a high-transmission-rate underwater optical wireless link with uplink and downlink transmissions.

Figure 1 illustrates the framework of the demonstrated 50 Gb/s PAM4 UWOC systems across the water–air–water interface. A pseudorandom bit sequence (PRBS) pattern generator with two output channels generates two binary PRBS data streams with an aligned clock at

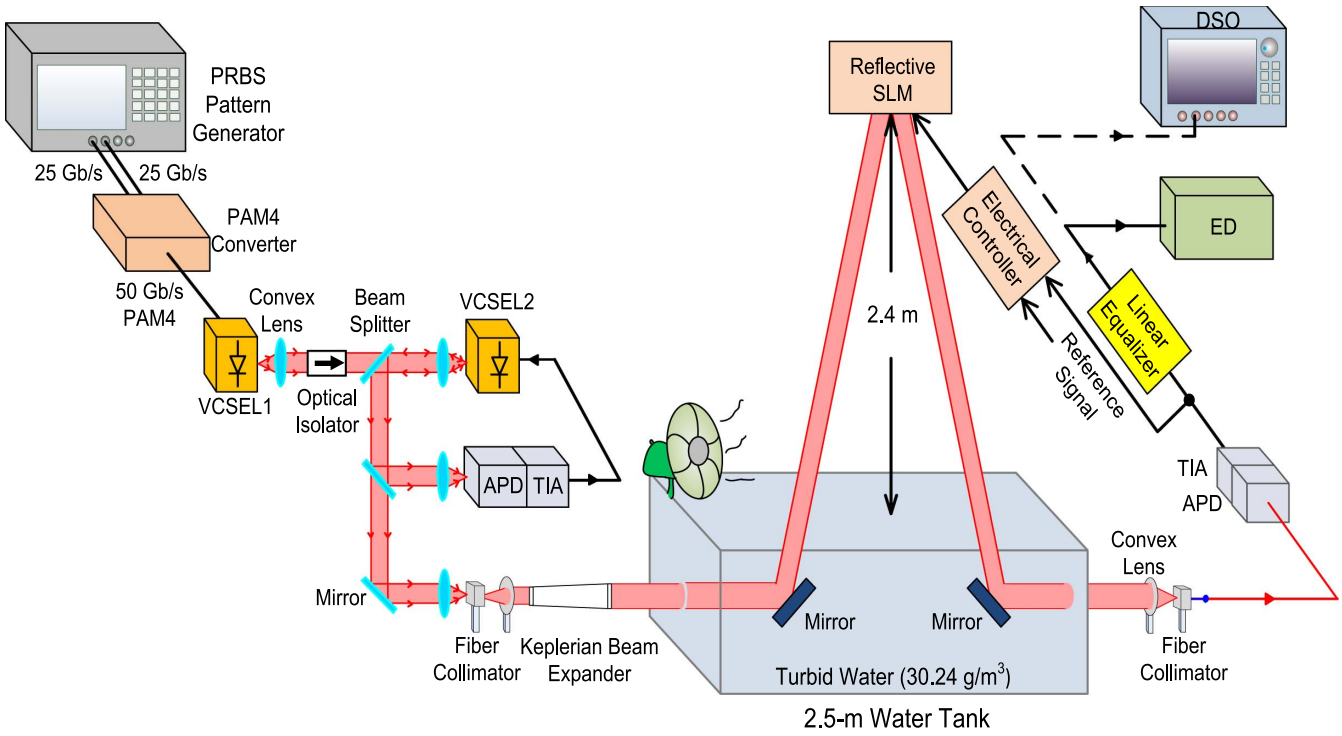

Fig. 1. Framework of demonstrated 50 Gb/s PAM4 UWOC systems across the water–air–water interface.

25 Gb/s with a length of $2^{15}-1$. Two binary PRBS data streams have amplitudes of 1.2 and 0.6 V, respectively. A PAM4 converter transforms two 25 Gb/s NRZ signals into a 50 Gb/s four-level PAM4 signal. A vertical-cavity surface-emitting laser-1 (VCSEL1), with a central wavelength and 3 dB bandwidth of 671.2 nm and 5.3 GHz, respectively, is directly driven by a 50 Gb/s PAM4 signal. PAM4 linearity is a vital factor for PAM4 VCSEL-based UWOC systems to directly modulate the VCSEL1. A linear driver should be deployed for the VCSEL to function in the linear region; however, given that the VCSEL's power-driving current curve approaches linear distribution, a linear driver is not required. VCSEL1's output is injected into VCSEL2. VCSEL1 and VCSEL2 have similar optical characteristics. A division of the laser beam is employed for the optoelectronic feedback loop, and another is utilized for the 50 Gb/s PAM4 UWOC systems. An avalanche photodiode (APD) with a transimpedance amplifier (TIA) receiver transforms the laser beam into a 50 Gb/s PAM4 signal to directly drive the VCSEL2. An optical isolator is employed to prevent the laser beam emitted from the VCSEL2. Several optical devices need to be deployed for light injection and the optoelectronic feedback scheme, including two VCSELs, three convex lenses, two beam splitters, one optical isolator, and one APD with a TIA receiver. Nevertheless, these optical devices are worth deploying because a VCSEL employing light injection and optoelectronic feedback techniques achieves a considerable 3 dB bandwidth improvement.

The laser beam emitted from the VCSEL2 with light injection and optoelectronic feedback techniques is sent to a Keplerian beam expander to spread the beam size and thus improve the performance of UWOC systems[14,15]. The expanded laser beam is delivered across a rectangular water tank with length × width × height of 2.5 m × 0.5 m × 0.5 m. The rectangular water tank is full of turbid water with a particle concentration of 30.24 g/m^3. The water turbidity is made with $Mg(OH)_2$ and $Al(OH)_3$ suspensions by increasing a commercial antacid preparation (Maalox)[16]. In turbid underwater links, the attenuation coefficient at 670 nm [2.1670 m^{-1} = 1.5059 m^{-1} (scattering coefficient) + 0.6611 m^{-1} (absorption coefficient)] is lower than that at 450 nm [2.8485 m^{-1} = 2.2756 m^{-1} (scattering coefficient) + 0.5729 m^{-1} (absorption coefficient)] or 520 nm [2.2973 m^{-1} = 1.9693 m^{-1} (scattering coefficient) + 0.3280 m^{-1} (absorption coefficient)][17]. With a low attenuation coefficient, the performance of PAM4 UWOC systems can be further enhanced because less light is attenuated by turbid water. A 670 nm red-light VCSEL transmitter is therefore adopted in a turbid water link, rather than a 450 nm blue-light or 520 nm green-light LD transmitter. Two plane mirrors are placed in the rectangular water tank at an inclined angle to reflect the laser beam across the water–air–water interface. A reflective SLM is placed above the water tank as a reflective mirror to reflect the laser beam and to perform uplink and downlink propagations. The vertical distance between the reflective SLM and the water tank is 2.4 m. A 4.9-m (2.45 m × 2) free-space transmission with a 0.9 m (0.45 m × 2) turbid underwater link is attainably constructed, with a total power loss of around 3.2 dB. The reflective SLM has a short response time and a high light operation efficiency. The high light operation efficiency primarily relies on reflectivity and diffraction loss. For the SLM utilized in this work, the response time is shorter than 5 ms, the reflectivity is

higher than 95%, and the diffraction loss is lower than 5%. Furthermore, given that the wind speed is 8–12 mph ($3.6-5.4$ m/s) for gentle breeze, an electric fan with a gentle breeze of ~5 m/s is utilized to simulate the natural wind in the environment. After reflection by the right-side plane mirror, the laser beam is concentrated by a convex lens, with a diameter of 35 mm, to guide it into the fiber collimator. A small coupling loss of 0.23 dB exists between the convex lens and the fiber collimator. A part of laser beam is received and boosted by a 25 GHz high-bandwidth APD with a TIA receiver, and another is supplied to an electrical controller to flexibly adjust the laser beam. The APD's single-mode fiber pigtail, with a length of 30 cm, is used to connect the fiber collimator. The boosted 50 Gb/s PAM4 signal is input into a linear equalizer for signal equalization, and then sent to a high-sensitivity error detector with a receiving sensitivity of 10 mV to enhance the BER measurement. In addition, a digital storage oscilloscope is employed to catch the eye diagrams of the transmitted 50 Gb/s PAM4 signal.

The reflective SLM with an electrical controller for developing a water–air–water interface and mitigating the performance degradation due to laser beam misalignment is shown in Fig. 2. The SLM has a spatial resolution of 1920×1080 pixels and a pixel size of 8 μm. It is based on liquid crystal on silicon technology in which liquid crystal is operated by a calculated voltage sent out from an electrical controller. The electrical controller is used to operate the liquid crystal inside the SLM when an arbitrary varying input signal reaches one of the inputs. It is utilized to compare two signals that are given at the two inputs. One is the reference signal and the other is the signal coming from the output of the APD with a TIA receiver.

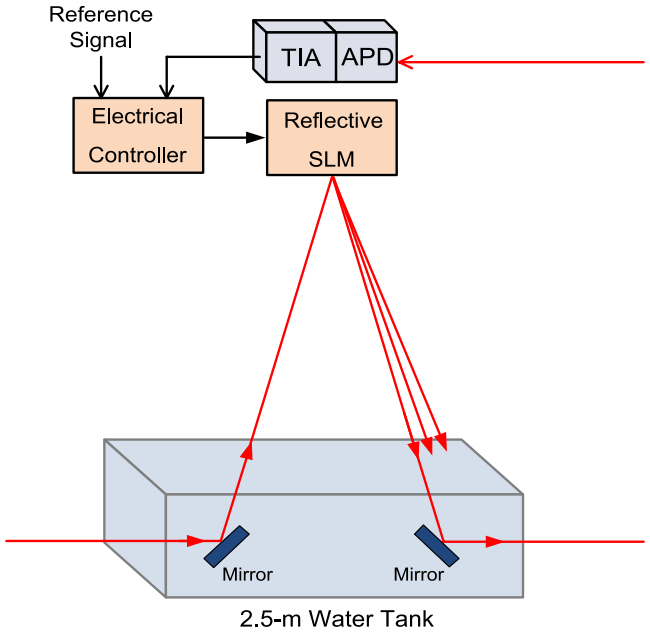

Fig. 2. Reflective SLM with an electrical controller for developing a water–air–water interface and mitigating the performance degradation due to laser beam misalignment.

Natural wind causes ocean ripple, brings on change in the laser beam's refraction angle, leads to the laser beam misalignment, and thereby results in less light received by the APD with a TIA receiver. The electrical controller takes two input signals, compares them, and gives a differential output voltage with either a high- or low-level signal. With the electrical controller, we can arbitrarily adapt the spatial light and relieve the laser beam misalignment induced by the natural wind. It is an effective method to control the spatial light by using the SLM with an electrical controller. With the adoption of a reflective SLM with an electrical controller, performance degradation due to natural wind in the environment can be mitigated. For a reflective SLM, zero-order diffraction efficiency is an important factor. Here, a mirror coating is put on a backplane to enhance the diffraction efficiency and thereby attain a high reflectivity (>95%) at 671 nm. Response time is another important factor for a reflective SLM. The SLM's response time is primarily restricted by that of the liquid crystal. Given that the natural wind speed is ~5 m/s, the reflective SLM's response time (<5 ms) can satisfy the requirement for adjusting the spatial light. Moreover, the wind speed is 25–31 mph (11–14 m/s) for a strong breeze. In a strong breeze scenario, the reflective SLM's response time can still meet the target for adjusting the spatial light. It indicates that wind variation has a very limited effect on the UWOC systems across the water–air–water interface.

There is no adaptive adjustment of the laser beam from the first (left-side) mirror to the reflective SLM. One of the challenges in UWOC systems is the ocean flow. Laser beam misalignment owing to ocean flow will cause link unreliability. However, a reflective SLM with an electrical controller can also be adopted as a flexible mirror to alleviate laser beam misalignment because of ocean flow.

The VCSEL2's optical spectrum with a free-running state is presented in Fig. 3(a). Figure 3(b) presents the VCSEL2's optical spectrum with light injection and optoelectronic feedback techniques locked at 671.2 nm. The injection-locked VCSEL2's optical spectrum moves to a somewhat longer wavelength (671.08 nm→671.2 nm). Light injection and optoelectronic feedback actions occur as the master laser (VCSEL1) is slightly detuned to a wavelength longer than that of the slave laser (VCSEL2). One significant attribute of injection locking is that the slave laser is forced to locate at the master laser's wavelength. Therefore, the wavelength component at the injection wavelength is influential. Moreover, it was found that the peak power and linewidth of the injection-locked VCSEL2 are enhanced and reduced to a certain extent. Employing light injection and optoelectronic feedback techniques increases the optical power and reduces the linewidth of the slave laser, resulting in an injection-locked slave laser with enhanced optical characteristics and a system with improved transmission performance.

Figure 4 displays the modulation responses of the free-running VCSEL under various operational currents. Modulation response is a vital figure-of-merit that characterizes the VCSEL's attribute. Given that the operational

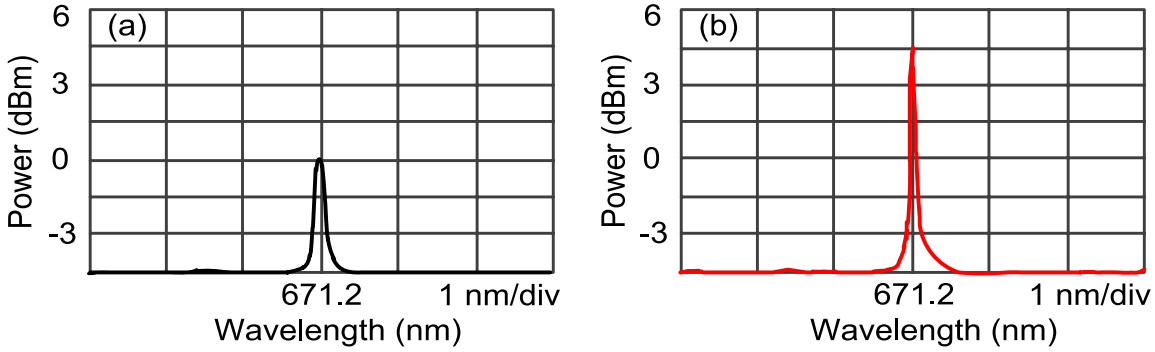

Fig. 3. Optical spectrum of VCSEL2 with (a) free-running state, and (b) light injection and optoelectronic feedback techniques locked at 671.2 nm.

current is 10.2 mA, the 3 dB modulation bandwidth reaches 5.3 GHz. The result shows that such a red-light VCSEL is intended for effective use in high-transmission-rate UWOC systems. Furthermore, the modulation responses of the VCSEL with light injection, and with light injection and optoelectronic feedback, are displayed in Fig. 4. Obviously, the modulation bandwidth can be up to 20.8 GHz. Light injection and optoelectronic feedback are acknowledged as one of the most effective approaches to enhancing the modulation bandwidth[18]. The modulation bandwidth can be considerably improved (5.3 GHz→20.8 GHz) by adopting light injection and optoelectronic feedback techniques. In addition, the modulation response is performed by a descent at the middle frequencies and a resonance peak at the high frequencies to attain a great 3 dB bandwidth improvement. Because 20.8 GHz is located at the resonance peak, the drop in the middle frequencies will not influence the transmission performance. Given that a VCSEL with light injection and optoelectronic feedback possesses a 20.8 GHz 3 dB modulation bandwidth, the maximum transmission capacity can reach 58.82 Gb/s ($20.8 \times \sqrt{2} \times 2 = 58.82$) by adopting PAM4 modulation. As for a noisy channel, the maximum transmission capacity will be lower than 58.82 Gb/s. Since 50 Gb/s is far lower than the related capacity of 58.82 Gb/s, a 50 Gb/s PAM4 UWOC link can be feasibly realized.

Figure 5 presents the BER performance of the 50 Gb/s PAM4 signal in the first 5 minutes for the states with or without a Keplerian beam expander or an SLM electrical controller. With a beam expander, but without an electrical controller, the BER reaches 5.2×10^{-9}. With a beam expander and an electrical controller, the BER slightly improves to 10^{-9} at a received optical power of 0.3 dBm. With an electrical controller, the performance decline due to laser beam misalignment can be alleviated. However, laser beam misalignment due to the natural wind in the environment in the first 5 minutes is trivially small. Therefore, the electrical controller only provides a small improvement to BER performance in the first 5 minutes. Additionally, it was observed that the BER degrades to 8.4×10^{-7} for the state without a beam expander but with an electrical controller. The BER further degrades to 8.7×10^{-7} for the state without a beam expander and an electrical controller. In turbid underwater links, the BER performance improves as the laser

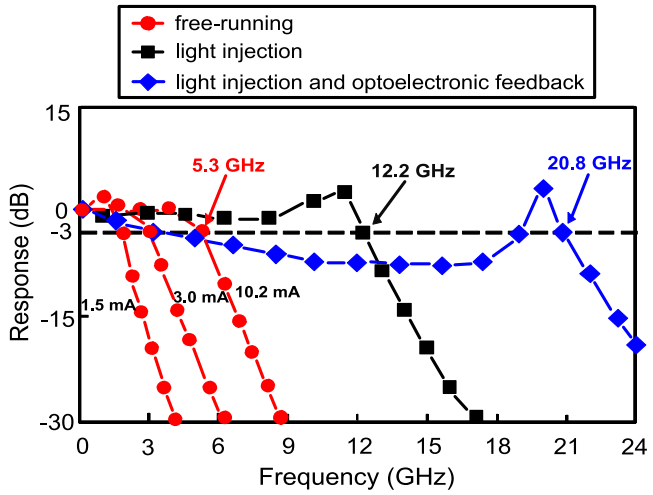

Fig. 4. Modulation responses of VCSEL with free-running (under various operational currents), light injection, and light injection and optoelectronic feedback.

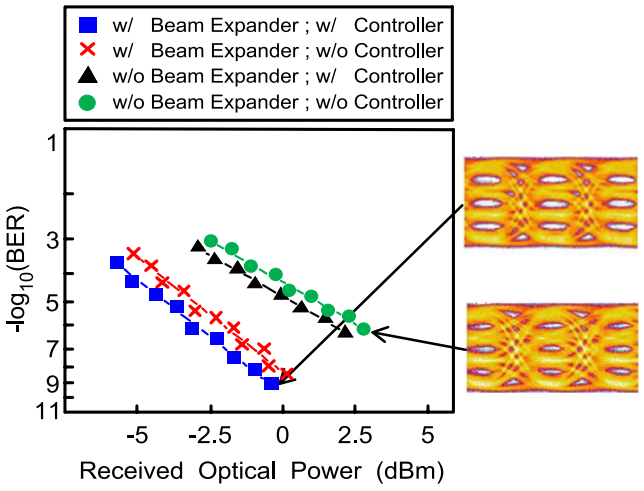

Fig. 5. BER performance of the 50 Gb/s PAM4 signal in the first 5 minutes for the states with or without a Keplerian beam expander or an SLM electrical controller.

beam size increases. The BER is significantly degraded without a Keplerian beam expander to spread the beam size. A smaller beam diameter that follows a larger beam divergence contributes less forward-scattered light to be accumulated by the fiber collimator and received by the APD with a TIA receiver, which results in poorer BER. In conclusion, with a beam expander (with a beam diameter of 8.7 mm and a scattering angle of 0.3°), the BER reaches a 10^{-9} order of magnitude; without a beam expander (with a beam diameter of 4.4 mm and a scattering angle of 0.36°), the BER degrades to a 10^{-7} order of magnitude. The beam diameters reaching the convex lens are 29.3 mm and 35.2 mm, respectively, in the conditions of with/without a beam expander. In the condition of without a beam expander, the diameter of the laser beam (35.2 mm) is larger than that of the convex lens (35 mm), and the APD with a TIA receiver receives less forward-scattered light, which leads to a higher BER. A Keplerian beam expander, rather than an SLM electrical controller, is an important contributor in turbid underwater links in the first 5 minutes.

In terms of PAM4 eye diagrams in the first 5 minutes, clear and open eye diagrams are achieved for the state with a beam expander and an electrical controller. Moreover, more or less clear eye diagrams are obtained for the state without a beam expander and an electrical controller.

Figure 6 exhibits the BER performance of the 50 Gb/s PAM4 signal in the first hour for the scenarios with or without a Keplerian beam expander or an SLM electrical controller. With an electrical controller and a beam expander, the BER reaches 10^{-9}. With an electrical controller but without a beam expander, the BER declines to 8.8×10^{-7}. In addition, it is to be found that the BER seriously declines to 4.6×10^{-4} for the state without an electrical controller, whether with or without a beam expander. The BER curves for the scenarios without an electrical controller are almost similar, revealing that the electrical controller is a vital contributor through a water–air–water interface. After 1 hour, laser beam misalignment because of natural wind in the environment becomes substantially large. By way of the electrical controller, the spatial light can be arbitrarily attuned to make up for the BER decline thanks to laser beam misalignment. After a period of time, therefore, the electrical controller provides a great improvement to the BER performance. To summarize, with an electrical controller, the BER reaches a $10^{-7}/10^{-9}$ order of magnitude; without an electrical controller, the BER seriously declines to a 10^{-4} order of magnitude. After a period of time, the SLM electrical controller, rather than a Keplerian beam expander, is a substantial contributor through the water–air–water interface.

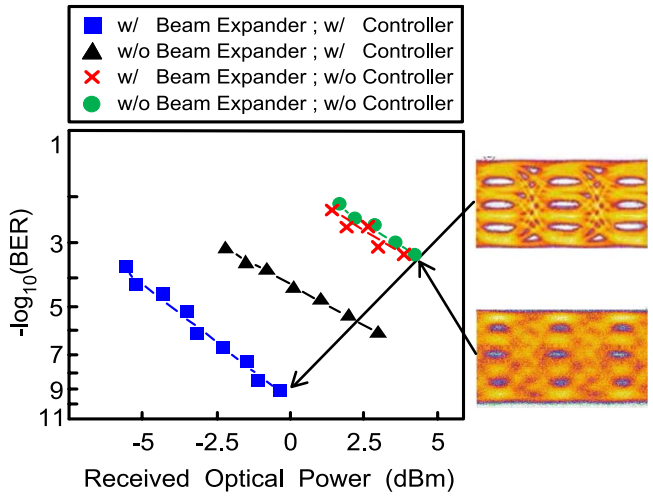

Fig. 6. BER performances of 50 Gb/s PAM4 signal in the first hour for the scenarios with or without a Keplerian beam expander or an SLM electrical controller.

Regarding the PAM4 eye diagrams, three independent clear eye diagrams are achieved for the condition with a beam expander and an electrical controller. For the condition without a beam expander and an electrical controller, however, turbid eye diagrams are acquired.

A 50 Gb/s PAM4 UWOC system across the water–air–water interface is successfully demonstrated for the first time. In an oceanic engineering scenario, laser beam misalignment on the account of natural wind in the environment induces performance decline and link unreliability. By adopting a reflective SLM with an electrical controller, not only can the laser beam be reflected to attain a practical water–air–water scenario, but oceanic engineering problems can also be solved to build a reliable UWOC link. After a period of time, a reflective SLM with an electrical controller provides a significant improvement to transmission performance. Impressive BER performance and clear PAM4 eye diagrams are acquired with the assistance of a Keplerian beam expander and an SLM electrical controller. The results demonstrate that the PAM4 UWOC system across the water–air–water interface exhibits a feasible state that outperforms current UWOC systems due to its attribute for affording a high-transmission-rate water–air–water link. Such innovative 50 Gb/s PAM4 UWOC systems through the water–air–water interface provide a practical scenario and a high-speed underwater link that can hasten the implementation of UWOC systems with an uplink from water to air and a downlink from air to water.

This work was financially supported by the Ministry of Science and Technology of Taiwan, China (MOST) (Nos. 107-2221-E-027-077-MY3 and 107-2221-E-027-078-MY3).

References

1. W. S. Tsai, H. H. Lu, H. W. Wu, C. W. Su, and Y. C. Huang, Sci. Rep. **9**, 8605 (2019).
2. X. Hong, C. Fei, G. Zhang, J. Du, and S. He, Opt. Lett. **44**, 558 (2019).
3. X. Liu, S. Yi, X. Zhou, S. Zhang, Z. Fang, Z. J. Qiu, L. Hu, C. Cong, L. Zheng, R. Liu, and P. Tian, Opt. Express **26**, 19260 (2018).
4. M. Kong, Y. Chen, R. Sarwar, B. Sun, Z. Xu, J. Han, J. Chen, H. Qin, and J. Xu, Opt. Express **26**, 3087 (2018).

5. C. Y. Li, H. H. Lu, Y. N. Chen, C. W. Su, Y. R. Wu, Z. H. Wang, and Y. P. Lin, IEEE Photonics J. **10**, 7906109 (2018).
6. C. Y. Li, H. H. Lu, W. S. Tsai, Z. H. Wang, C. W. Hung, C. W. Su, and Y. F. Lu, IEEE Photonics J. **10**, 7904809 (2018).
7. S. M. Kim, J. Choi, and H. Jung, Chin. Opt. Lett. **16**, 080101 (2018).
8. A. Wang, L. Zhu, Y. Zhao, S. Li, W. Lv, J. Xu, and J. Wang, Opt. Express **26**, 8669 (2018).
9. M. S. Islam, M. Younis, and A. Ahmed, in *IEEE International Conference on Communication (ICC)* (2018), p. 1.
10. J. Harriman, S. Serati, and J. Stockley, Proc. SPIE **5930**, 59302D (2005).
11. H. M. Oubei, E. Zedini, R. T. ElAfandy, A. Kammoun, M. Abdallah, T. K. Ng, M. Hamdi, M. S. Alouini, and B. S. Ooi, Opt. Lett. **42**, 2455 (2017).
12. Y. Chen, M. Kong, T. Ali, J. Wang, R. Sarwar, J. Han, C. Guo, B. Sun, N. Deng, and J. Xu, Opt. Express **25**, 14760 (2017).
13. J. Wang, C. Lu, S. Li, and Z. Xu, Opt. Express **27**, 12171 (2019).
14. H. M. Oubei, R. T. ElAfandy, K. H. Park, T. K. Ng, M. S. Alouini, and B. S. Ooi, IEEE Photonics J. **9**, 7903009 (2017).
15. B. M. Cochenour, L. J. Mullen, and A. E. Laux, IEEE J. Oceanic Eng. **33**, 513 (2008).
16. M. Pittol, D. Tomacheski, D. N. Simões, V. F. Ribeiro, and R. M. C. Santana, Plast. Rubber Compos. **46**, 223 (2017).
17. L. Prieur and S. Sathyendranath, Limnol. Oceanogr. **26**, 671 (1981).
18. H. H. Lu, C. Y. Li, H. W. Chen, Z. Y. Yang, X. Y. Lin, M. T. Cheng, C. K. Lu, and T. T. Shih, Opt. Lett. **41**, 5023 (2016).